

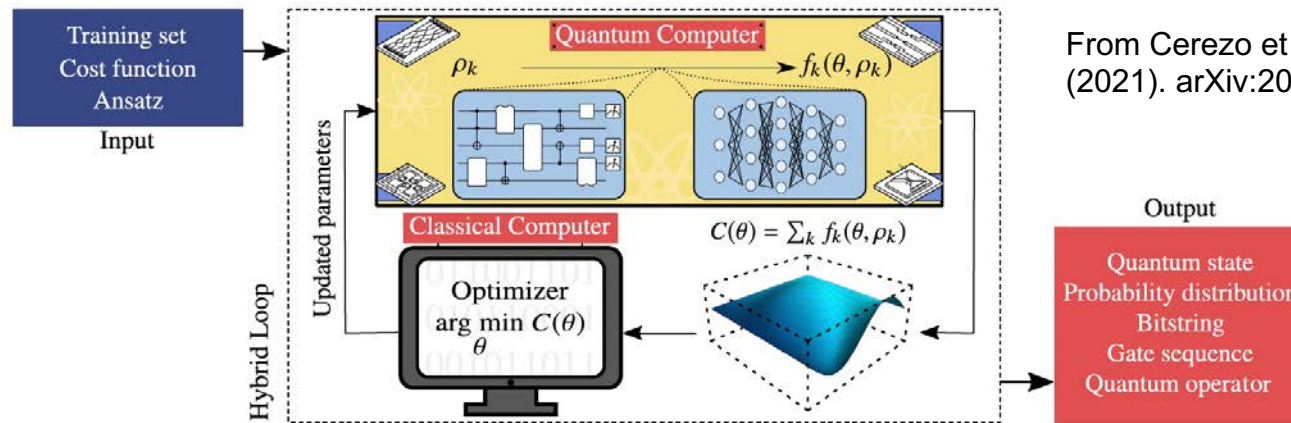
Variational quantum algorithms 1

Peter P. Orth (Iowa State University & Ames Laboratory)



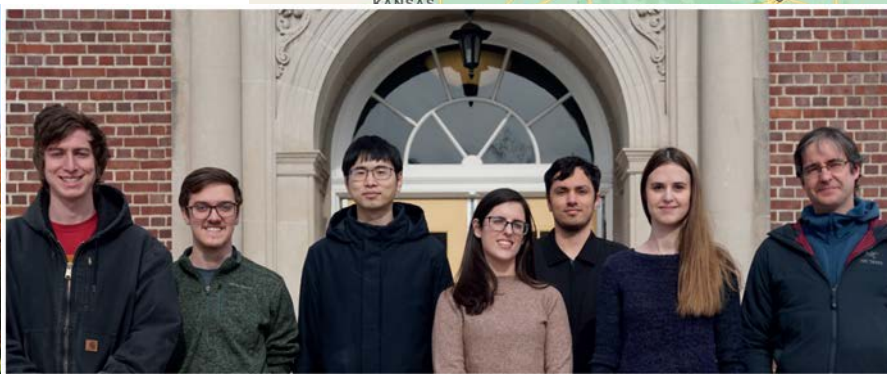
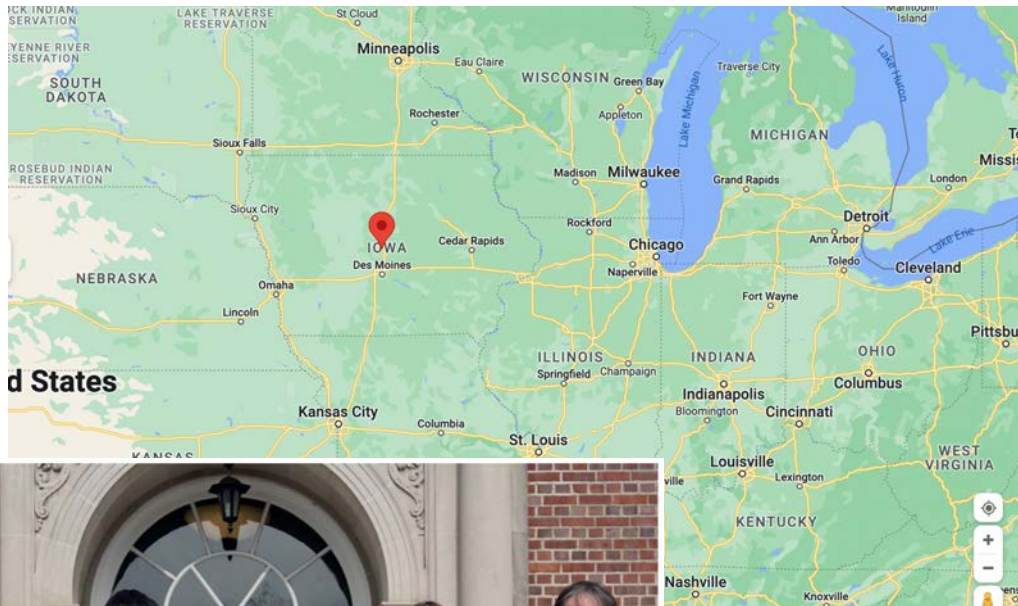
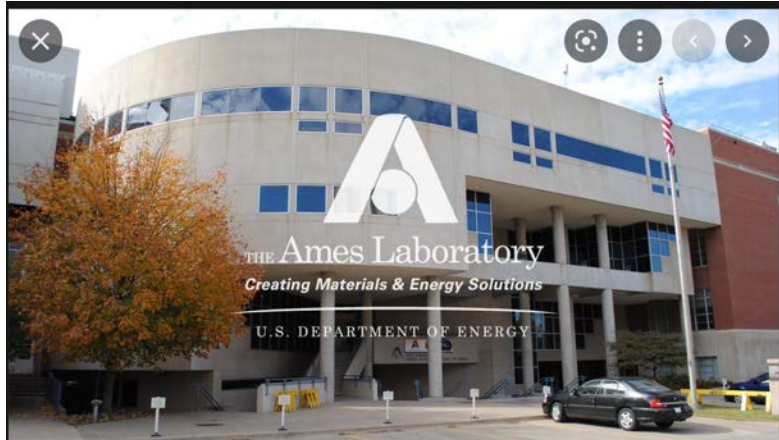
Office of Science

SQMS/GGI Summer School, Florence, Italy, 26 July 2022



From Cerezo et al., Nat. Phys. Reviews (2021). arXiv:2012.09265

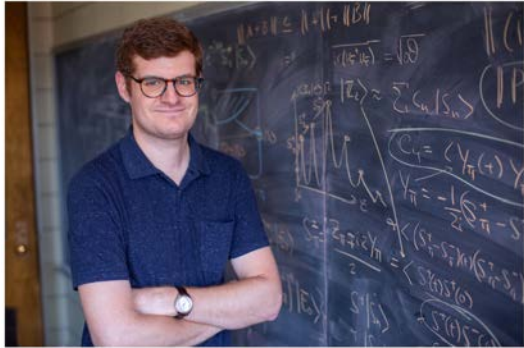
Ames National Lab & Iowa State University



(Part of) my group earlier this year

Check out:
www.physastro.iastate.edu

Quantum Computing at Ames National Laboratory & Iowa State



Thomas Iadecola studies how states of matter emerge from collections of atoms and subatomic particles and recently contributed theoretical work and data analysis to a paper published by the journal Nature. [Larger photo](#). Photo by Christopher Gannon.



Srimoyee Sen

Tom Iadecola (Nonequilibrium dynamics, topological field theory, quantum computing)

Srimoyee Sen (QCD, quantum field theory)

- > Ames Lab participates in two national quantum initiative centers of the Department of Energy (SQMS & C2QA)
- > Strong collaborations across fields and between theory and experiment at Ames National Lab



Yongxin Yao (materials simulations, quantum computing)

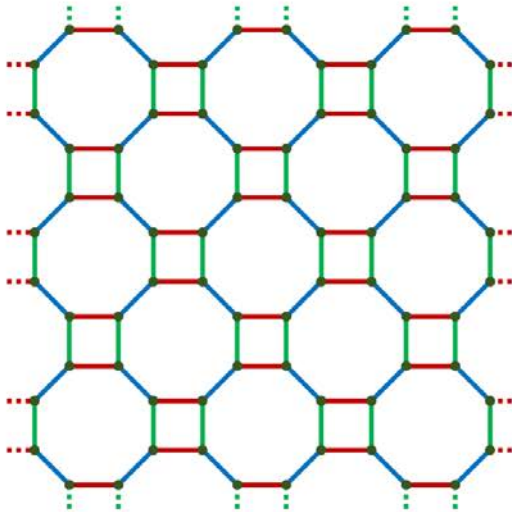


Joint group meeting of my group and the groups of Prof. Flint and Prof. Iadecola

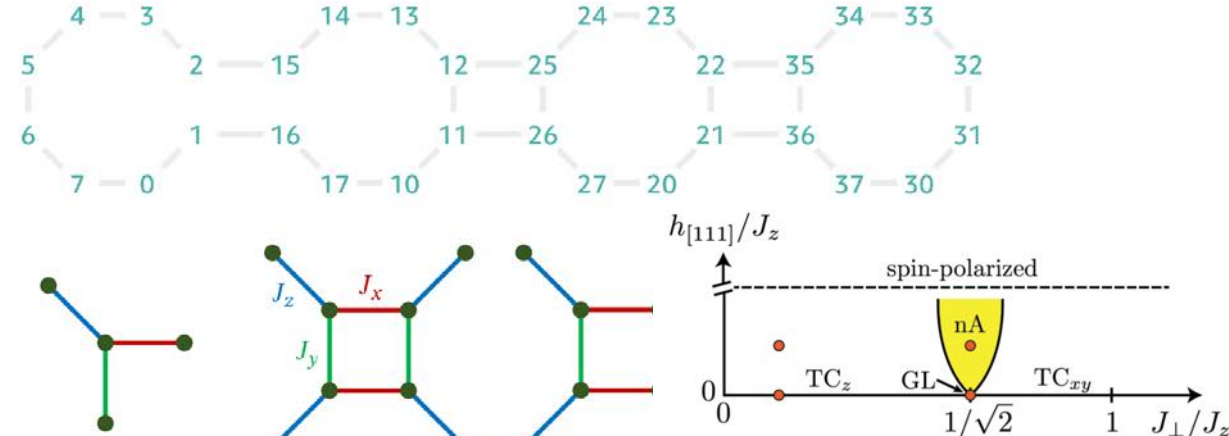
VQE for Kitaev spin model

From:
Li et al. (SQMS), arXiv (2021)

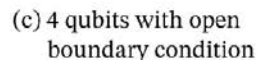
(a) Square-octagon lattice



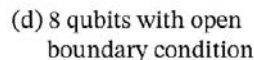
(b) Aspen-9 Rigetti QPU



(c) 4 qubits with open boundary condition



(d) 8 qubits with open boundary condition



Kitaev model on square-octagon lattice matches Rigetti's QPU geometry. No SWAP gates needed as connectivities match.

(e) FIG. 2. Phase Diagram. Schematic phase diagram of the Kitaev model (2.2) on the square-octagon lattice as a function of spin exchange anisotropy J_\perp/J_z with $J_\perp \equiv J_x = J_y$ and magnetic field in [111] direction $h_{[111]}$. It includes gapped toric code phases (TC_z , TC_{xy}) that are stable with respect to small fields, the gapless line (GL) at $J_\perp/J_z = 1/\sqrt{2}$ and a phase with non-Abelian (nA) Majorana excitations that emerges in field above the gapless line. At large magnetic fields the system enters a spin-polarized paramagnetic phase. The red circles denote the different, representative model parameter points that are studied in our benchmark simulations.

VQE ansatz

From:
Li et al. (SQMS), arXiv (2021)

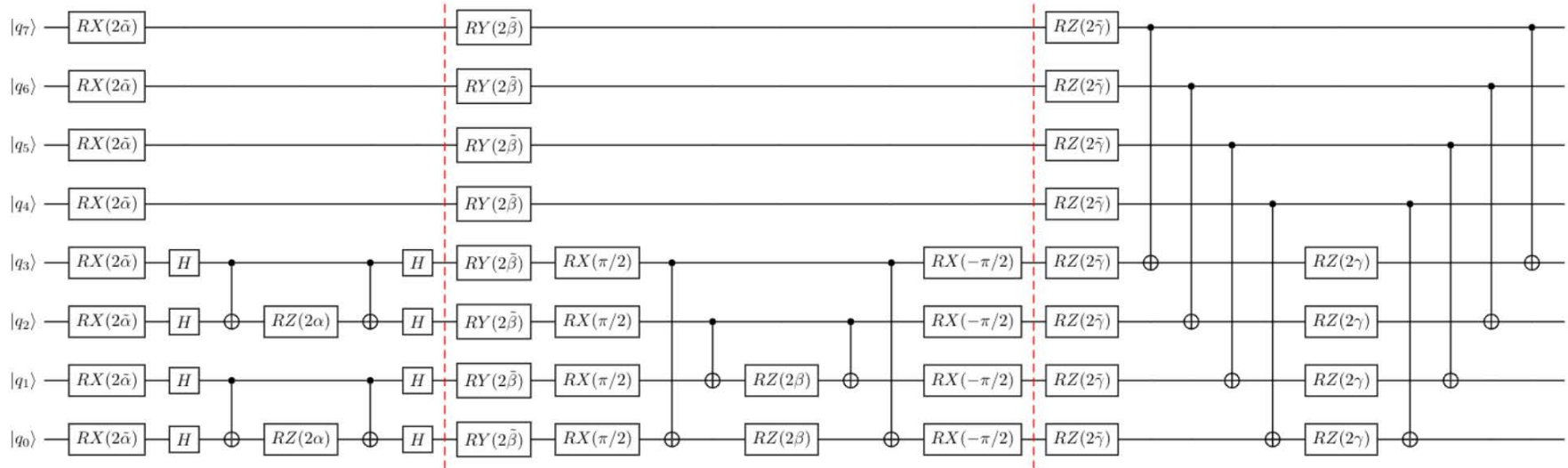
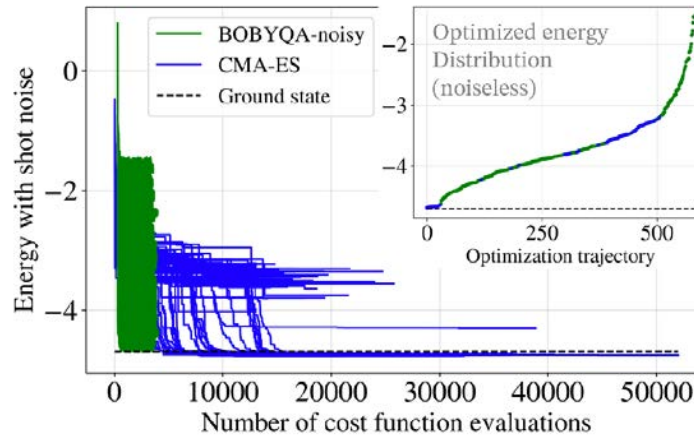
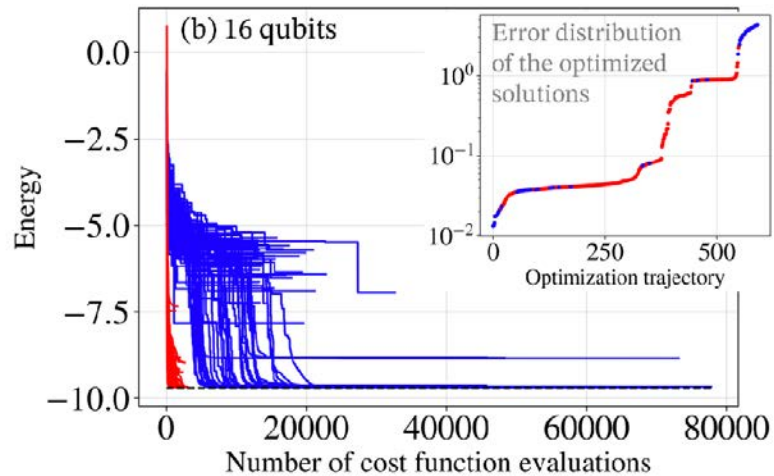


FIG. 3. HVA with one layer on eight qubits. The Hamiltonian Variational Ansatz (HVA) with one layer on eight qubits, split into commuting blocks. The first block corresponds to the operation $e^{-i\bar{\alpha}\sum_q X_q} e^{-i\alpha\sum_{(i,j)\in X\text{-links}} X_i X_j}$, the second to $e^{-i\bar{\beta}\sum_q Y_q} e^{-i\beta\sum_{(i,j)\in Y\text{-links}} Y_i Y_j}$, and the third to $e^{-i\bar{\gamma}\sum_q Z_q} e^{-i\gamma\sum_{(i,j)\in Z\text{-links}} Z_i Z_j}$. For the circuit shown here, we used $X\text{-links} = \{(q_0, q_1), (q_2, q_3)\}$, $Y\text{-links} = \{(q_0, q_3), (q_1, q_2)\}$, and $Z\text{-links} = \{(q_0, q_4), (q_1, q_5), (q_2, q_6), (q_3, q_7)\}$.

Noiseless and noisy (shots) VQE optimization

From:
Li et al. (SQMS), arXiv (2021)



Noiseless: 16 qubits
Noisy: 8 qubits (8000 shots)

Optimizer	Error (noiseless)	Measured deviation	Cost function evaluations
BFGS, 501 initial values	0.45069	0.42052	mean: 747, max: 1994
BOBYQA, 501 initial values	0.27485	0.21843	mean: 471, max: 610
BOBYQA-noisy, 501 initial values	0.07989	-0.00453	mean: 3532, max: 4004
CMA-ES	0.02416	-0.06462	37570
CMA-ES, 80 initial values	0.01610	-0.07125	mean: 21042, max: 52000
Dual annealing	0.04534	-0.01631	60101
SPSA	0.00612	0.00879	100000 (cutoff)

Quantum circuits for measurement of $\text{Re}[G]$ and energy gradient

(a)

$$\text{Re} \left[\frac{\partial \langle \Psi[\theta] |}{\partial \theta_\mu} \frac{\partial |\Psi[\theta]\rangle}{\partial \theta_\nu} \right]$$

$\mu < \nu:$

$$\text{Re} \left[\langle \emptyset | \hat{U}_{0,\nu-1}^\dagger \hat{\mathcal{A}}_\nu \hat{U}_{\mu,\nu-1} \hat{\mathcal{A}}_\mu \hat{U}_{0,\mu-1} | \emptyset \rangle \right]$$

(b)

$$\text{Im} \left[\frac{\partial \langle \Psi[\theta] |}{\partial \theta_\mu} \hat{\mathcal{H}} |\Psi[\theta]\rangle \right]$$

$\mu < N_\theta - 1:$

$$\text{Re} \left[\langle \emptyset | \hat{U}_{0,N_\theta-1}^\dagger \hat{\mathcal{H}} \hat{U}_{\mu,N_\theta-1} \hat{\mathcal{A}}_\mu \hat{U}_{0,\mu-1} | \emptyset \rangle \right]$$

$\mu = N_\theta - 1:$

$$\text{Re} \left[\langle \emptyset | \hat{U}_{0,N_\theta-1}^\dagger \hat{\mathcal{A}}_\mu \hat{\mathcal{H}} \hat{U}_{0,N_\theta-1} | \emptyset \rangle \right]$$

(c)

$$\frac{\partial \langle \Psi[\theta] |}{\partial \theta_\mu} |\Psi[\theta]\rangle$$

$$i \langle \emptyset | \hat{U}_{0,\mu-1}^\dagger \hat{\mathcal{A}}_\mu \hat{U}_{0,\mu-1} | \emptyset \rangle$$

$$\langle \Psi[\theta] | \hat{\mathcal{H}} |\Psi[\theta]\rangle$$

$$\langle \Psi[\theta] | \hat{\mathcal{H}}^2 |\Psi[\theta]\rangle$$

Ancilla Register Register

$|0\rangle$ H X \cdot X \cdot H $\cancel{\chi}$

$|0\rangle$ $\hat{U}_A[\theta]$ $\hat{\sigma}_A$ $\hat{U}_B[\theta]$ $\hat{\sigma}_B$

$|0\rangle$ \vdots \vdots

$|0\rangle$ $H(S^\dagger)$ $\cancel{\chi}$

$|0\rangle$ $H(S^\dagger)$ $\cancel{\chi}$

$|0\rangle$ $H(S^\dagger)$ $\cancel{\chi}$

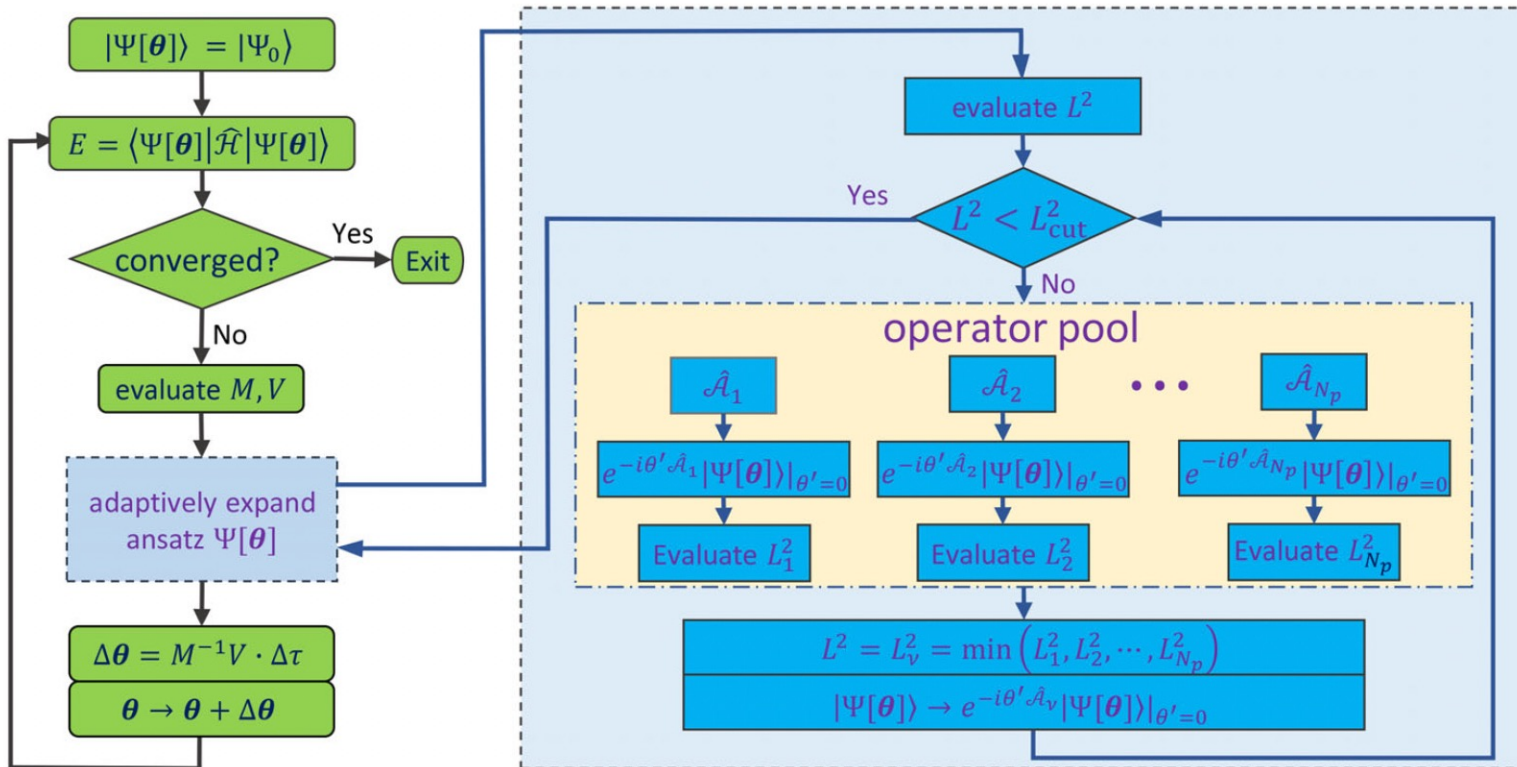
$|0\rangle$ \vdots \vdots

$|0\rangle$ $H(S^\dagger)$ $\cancel{\chi}$

From:
Yao, ...,
PPO, PRX
Quantum
(2021).

These circuits are for real-time evolution. For imaginary time evolution one applies an additional S^\dagger gate after the first Hadamard gate (and removes the X gates) in order to measure the imaginary part in the Hadamard test.

Adaptive variational quantum imaginary time evolution



From:
Gomes,
..., PPO,
Yao, Adv.
Qu. Tech
(2021).

Adaptive variational quantum imaginary time evolution

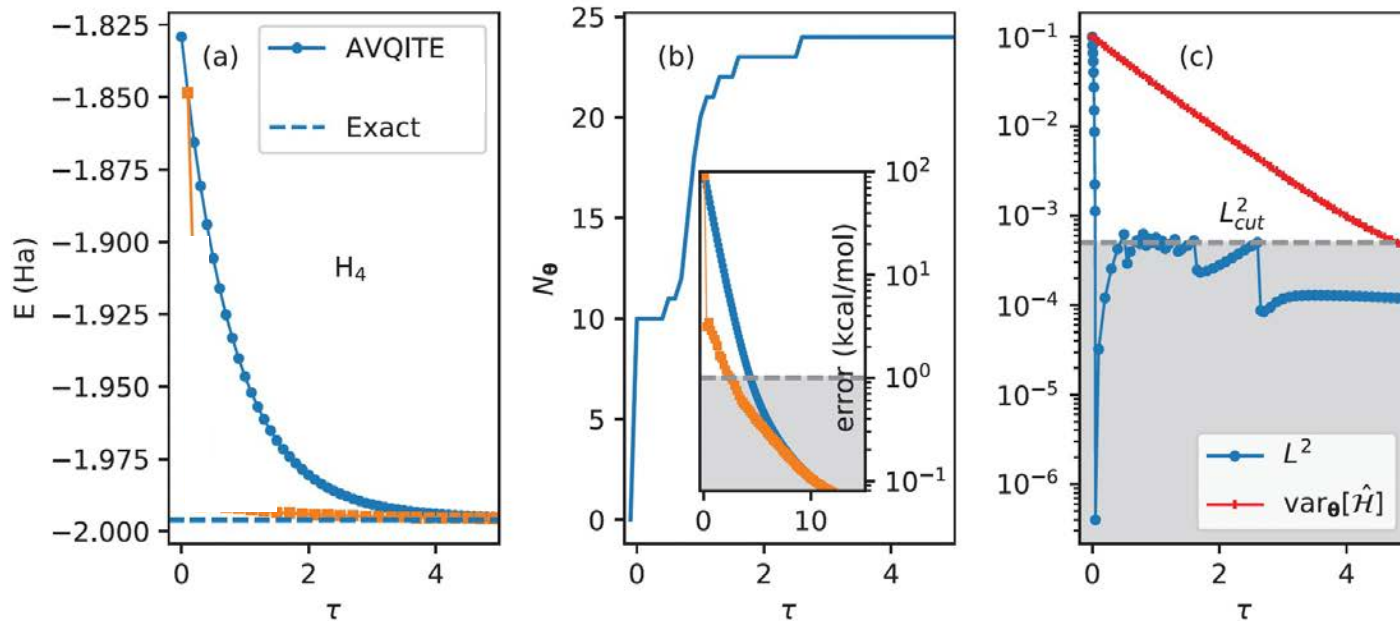


Figure 2. AVQITE calculation for H_4 chain. Along the imaginary time path of $\tau = N\Delta\tau$, the total energies of H_4 from AVQITE and quantum Lanczos calculations are shown in panel (a), the number of variational parameters N_θ in (b), and the McLachlan distance L^2 and energy variance $\text{var}_\theta[\hat{H}]$ in (c). The exact full configuration interaction result is shown as the dashed line in (a) for reference. The total energy errors $E - E_{\text{Exact}}$ are plotted in the inset of (b), with the shaded area denoting chemical accuracy. The chosen threshold $L^2_{\text{cut}} = 5 \times 10^{-4}$ is indicated by a dashed line in (c).

From:
Gomes,
..., PPO,
Yao, Adv.
Qu. Tech
(2021).

Time-dependent variational quantum algorithms

Variational form of quantum state

$$|\Psi[\theta]\rangle = \prod_{\mu=0}^{N_\theta-1} e^{-i\theta_\mu \hat{A}_\mu} |\Psi_0\rangle.$$

Variational parameters evolve in time

Von Neumann equation

$$\frac{d\rho}{dt} = \mathcal{L}(\rho) = -i[\mathcal{H}, \rho]$$

MacLachlan distance b/w exact
and variational time evolution

$$\begin{aligned} L^2 &\equiv \left\| \sum_{\mu} \frac{\partial \rho[\theta]}{\partial \theta_{\mu}} \dot{\theta}_{\mu} - \mathcal{L}[\rho] \right\|^2 \\ &= \sum_{\mu\nu} M_{\mu\nu} \dot{\theta}_{\mu} \dot{\theta}_{\nu} - 2 \sum_{\mu} V_{\mu} \dot{\theta}_{\mu} + \text{Tr} [\mathcal{L}[\rho]^2]. \end{aligned}$$

EOM for variational parameters

$$\sum_{\nu} M_{\mu\nu} \dot{\theta}_{\nu} = V_{\mu}.$$

Matrix $M_{\mu\nu}$ and vector V_{μ} measured on QPU

Minimize L^2

$$M_{\mu\nu} \equiv \text{Tr} \left[\frac{\partial \rho[\theta]}{\partial \theta_{\mu}} \frac{\partial \rho[\theta]}{\partial \theta_{\nu}} \right]$$

$$V_{\mu} \equiv \text{Tr} \left[\frac{\partial \rho[\theta]}{\partial \theta_{\mu}} \mathcal{L}[\rho] \right]$$

Only so good as the ansatz can follow the dynamics

☞ How to select an efficient yet flexible variational ansatz?

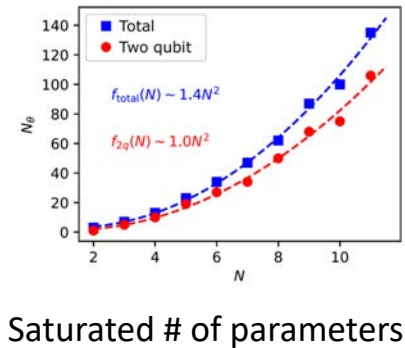
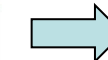
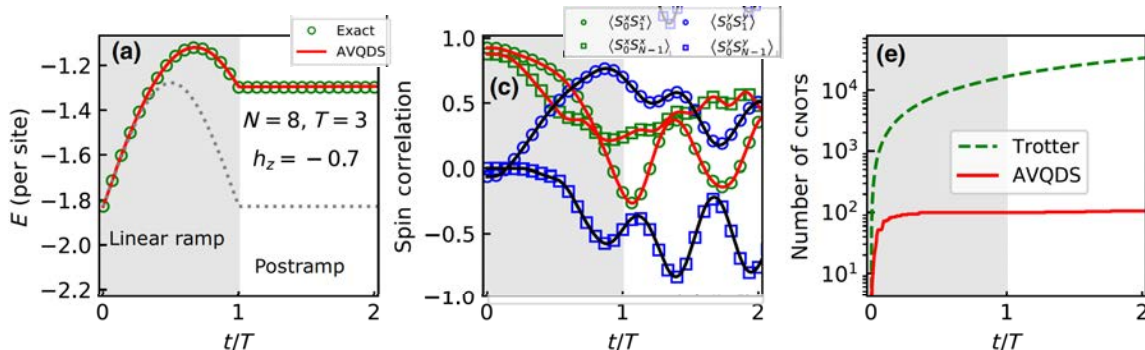
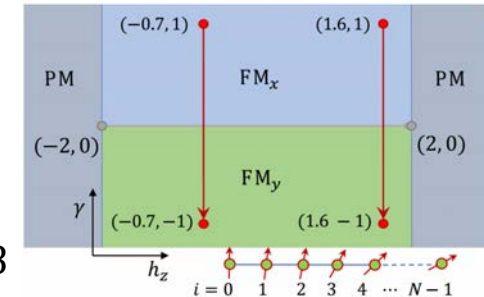
[1] Li, Benjamin, Endo, Yuan (2019).

Application I: continuous quench in integrable spin chain

- > Linear quench of anisotropic XY chain in transverse magnetic field

$$\hat{\mathcal{H}} = -J \sum_{i=0}^{N-2} \left[(1 + \gamma) \hat{X}_i \hat{X}_{i+1} + (1 - \gamma) \hat{Y}_i \hat{Y}_{i+1} \right] + h_z \sum_{i=0}^{N-1} \hat{Z}_i \quad \text{with} \quad \gamma(t) = 1 - \frac{2t}{T}$$

- > AVQDS follows exact solution during and after quench, shown for $N = 8$
- > Circuit depth saturates at 100 CNOTs << Trotter circuit depth 10^4 CNOTs
- > Can simulate system with gate depth **independent** of time t ↗ can simulate to arbitrary times!



Application II: sudden quench in nonintegrable spin chain

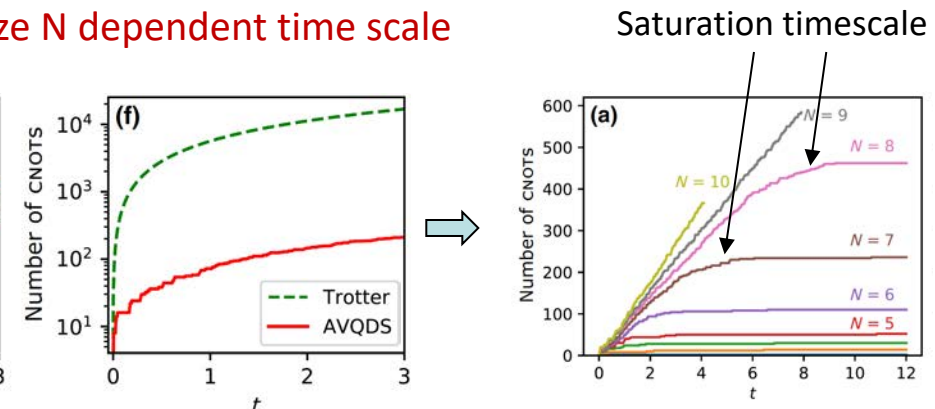
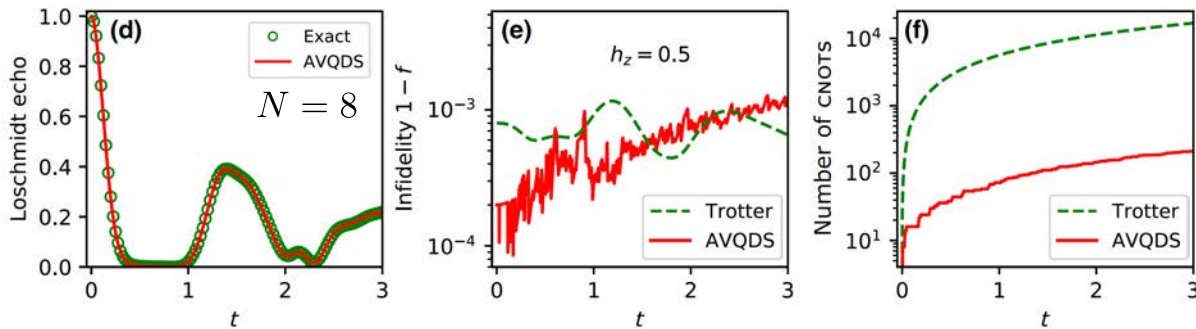
- > Sudden quench in mixed-field Ising model

$$\hat{\mathcal{H}} = -J \sum_{i=0}^{N-1} \hat{Z}_i \hat{Z}_{i+1} + \sum_{i=0}^{N-1} (h_x \hat{X}_i + h_z \hat{Z}_i)$$

Loschmidt echo: $\mathcal{L}(t) = \left| \langle \Psi_0 | e^{-i\hat{\mathcal{H}}_f t} | \Psi_0 \rangle \right|^2$

Initial state: $|\Psi_0\rangle = |\uparrow \cdots \uparrow\rangle$

- > AVQDS follows exact solution, shown for $N \leq 10$
- > Circuit depth two orders of magnitude smaller than Trotter circuit depth
- > AVQDS circuit depth saturates at system size N dependent time scale



Application II: sudden quench in nonintegrable spin chain

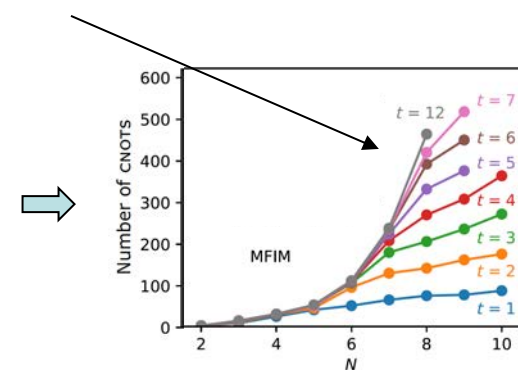
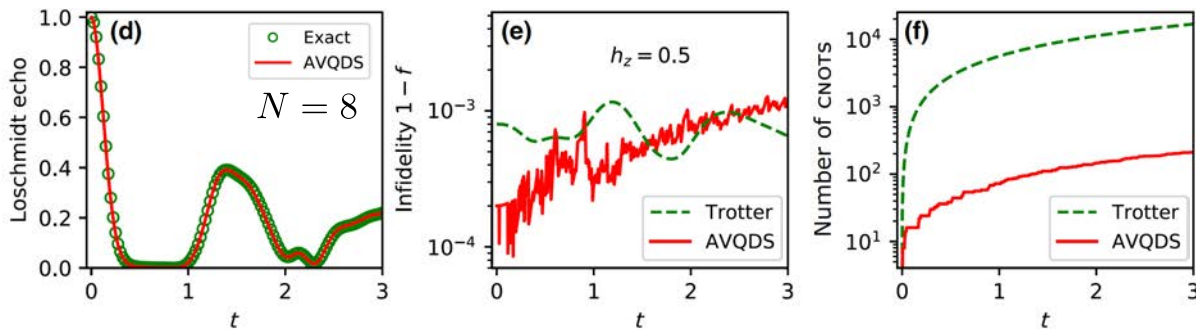
- > Sudden quench in mixed-field Ising model

$$\hat{\mathcal{H}} = -J \sum_{i=0}^{N-1} \hat{Z}_i \hat{Z}_{i+1} + \sum_{i=0}^{N-1} (h_x \hat{X}_i + h_z \hat{Z}_i)$$

Loschmidt echo: $\mathcal{L}(t) = \left| \langle \Psi_0 | e^{-i\hat{\mathcal{H}}_f t} | \Psi_0 \rangle \right|^2$

Initial state: $|\Psi_0\rangle = |\uparrow \cdots \uparrow\rangle$

- > Circuit depth two orders of magnitude smaller than Trotter circuit depth
- > Saturated AVQDS circuit depth scales exponentially with system size N
- > # measurements is main bottleneck of algorithm



VQE-X: variational quantum eigensolver for highly excited states

Adaptive variational quantum eigensolver for excited states

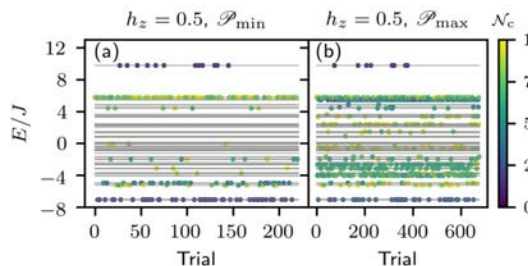
- > Long-time dynamics of observable determined by diagonal ensemble of excited states

$$\langle \mathcal{O}(t) \rangle = \sum_{n,m} c_n c_m^* e^{i(E_m - E_n)t} \langle m | \mathcal{O} | n \rangle \xrightarrow{t \rightarrow \infty} \langle \mathcal{O}(t) \rangle \approx \sum_n |c_n|^2 \langle n | \mathcal{O} | n \rangle$$

- > Adaptive variational quantum eigensolver to prepare highly excited states (VQE-X)

> Minimize energy variance (instead of energy):

$$\mathcal{C}(|\psi(\theta)\rangle) = \langle \psi(\theta) | H^2 | \psi(\theta) \rangle - \langle \psi(\theta) | H | \psi(\theta) \rangle^2$$

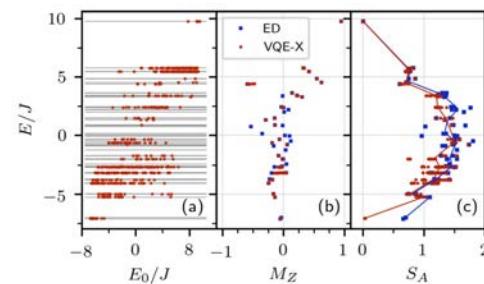
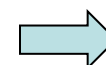


Full coverage of energy spectrum
for operator pool with long-
range Pauli strings

Nontrivial pool
dependence

$$\mathcal{P}_{\min} = \{Y_i\}_{i=1}^N \cup \{Y_i Z_{i+1}\}_{i=1}^N$$
$$\mathcal{P}_{\max} = \{Y_i\}_{i=1}^N \cup \{Y_i Z_j\}_{i,j=1}^N \cup \{Y_i X_j\}_{i,j=1}^N$$

[1] Zhang, Gomes, Yao, PPO, Iadecola,
PRB **104**, 075159 (2021).



Can investigate properties of volume
law highly excited states

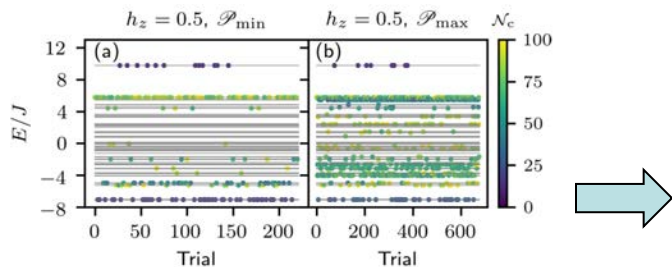
Adaptive variational quantum eigensolver for excited states

- > Long-time dynamics of observable determined by diagonal ensemble of excited states

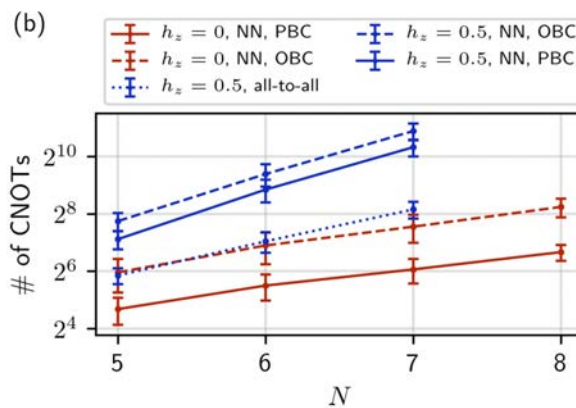
$$\langle \mathcal{O}(t) \rangle = \sum_{n,m} c_n c_m^* e^{i(E_m - E_n)t} \langle m | \mathcal{O} | n \rangle \xrightarrow{t \rightarrow \infty} \langle \mathcal{O}(t) \rangle \approx \sum_n |c_n|^2 \langle n | \mathcal{O} | n \rangle$$

- > Adaptive variational quantum eigensolver to prepare highly excited states (VQE-X)

> Minimize energy variance (instead of energy): $\mathcal{C}(|\psi(\theta)\rangle) = \langle \psi(\theta) | H^2 | \psi(\theta) \rangle - \langle \psi(\theta) | H | \psi(\theta) \rangle^2$



Full coverage of energy spectrum for operator pool with long-range Pauli strings



Exponential scaling of # CNOTs with system size
☞ relax convergence condition to represent microcanonical averages instead [1]

[1] Banuls, Huse, Cirac (2020)

Summary and outlook

- > Adaptive variational quantum dynamics simulation (AVQDS) framework
 - > Orders of magnitude shallower circuits than Trotter simulations
 - > Linear growth of # CNOTs with time initially, then saturation at e^N number of gates
 - > Allows simulation out to arbitrary times for small systems
- > Adaptive variational quantum eigensolver for highly excited states (adaptive VQE-X)
 - > Minimize energy variance allows preparing arbitrary excited states
 - > Generate volume-law states requires exponentially many parameters
 - > May be alleviated in simulations of microcanonical averages

References:

- N. Gomes *et al.*, arXiv:2102.01544 (2021)
- Y. Yao *et al.*, PRX Quantum **2**, 030307 (2021)
- F. Zhang *et al.*, PRB **104**, 075159 (2021)

Thank you for your attention!

